A 3D Printed Filtering Waveguide with Simple Metamaterial Construction

Zi-Yu Pang [1], Xiao-Yu Ma [1], Ge Zhao [1], Jia-Jun Liang [4*], Guan-Long Huang [1,2,3*], Luyu Zhao [5], and Chow-Yen-Desmond Sim [6]

[1] College of Electronics and Information Engineering
Shenzhen University, Shenzhen, Guangdong 518060, China
*guanlong.huang@ieee.org

[2] State Key Laboratory of Millimeter Waves, Nanjing, Jiangsu 210096, P.R. China

[3] Peng Cheng Laboratory, No.2 Xingke 1st Street, Nanshan, Shenzhen, Guangdong 518052, China

[4] School of Physics and Telecommunication Engineering
Yulin Normal University, Yulin, P.R. China
*shuigpjd@163.com

[5] National Key Laboratory of Antennas and Microwave Technology
Xidian University, Xi'an, Shaanxi, 710071, P.R. China

[6] Department of Electrical Engineering
Feng Chia University, Taichung 40724, Taiwan

Abstract ─ A novel filtering waveguide with bandwidth controllable characteristic is proposed in this work. The filtering waveguide consists of a common rectangular waveguide and metamaterial-based metallic bars. The proposed waveguide is designed for Ku-band application. Inside the operational frequency band, the metallic bars forming a metamaterial surface can behave as perfect electric conductor (PEC), which generates a pass-band for signal transmission, while outside the band of interest, the metallic bars act as perfect magnetic conductor (PMC) and block the transmission of undesired signals, where a stop-band is formed. After integrating the pass-band and stop-band features into the waveguide, a customized waveguide with filtering response is realized. A prototype of the proposed filtering waveguide is fabricated with the advanced metallic 3D printing technique, and experimental results well verify the desired performance. Moreover, the pass-band and stop-band of the filtering waveguide can be flexibly and easily adjusted to meet different requirements with low insertion loss.

Index Terms ─ Bandwidth controllable, filtering waveguide, low loss, metamaterial.

I. INTRODUCTION

With the development of wireless communication, high-frequency devices are always desired to be highly-integrated and versatile with compact size and lightweight. As two important microwave components, waveguide-based antennas and filters are frequently employed in advanced wireless systems like radar and satellite [1]-[7], where the filters are usually cascaded behind the antennas via waveguide connection. However, such traditional ways for cascading different components with waveguides result in a bulky size of the hardware system, which fails to meet the current wireless development requirements. Therefore, it is necessary to investigate multi-functional devices in a high-integration level. Waveguides integrated with filtering function are one of these devices and continually playing an important role in modern communication systems due to their unique radio-frequency (RF) advantages such as low insertion loss and high-power handling capabilities [8]. However, it is always challenging to realize such versatile three-dimensional components in a simple way.

Metamaterial is an artificial material proposed decades ago. It typically consists of a series of periodic electromagnetic (EM) structures or unit cells that can change the characteristics of incident electromagnetic waves, such as the direction of propagation, wave number and phase [9]. In recent years, the application of metamaterial structures to achieve filtering response in various microwave devices becomes a hot topic. Different methods for designing filtering structures with metamaterial have also been widely studied. For

Submitted On: February 1, 2020
Accepted On: April 5, 2020

example, a magnetic wall made of mushroom-shaped metamaterial was added into rectangular waveguide [10], [11], the analysis of which shows that the critical frequency of such a waveguide depends on the metamaterial resonance frequency and is close to 4 GHz, where the considered structure acts as waveguide filter and provides 500 MHz stop-band with rejection level of 21~24 dB. Although it could perform filtering function in a waveguide, this structure is too complicated to realize and had a relatively large insertion loss. Recently, a design approach of a waveguide slot filtering antenna array was proposed [12]. In this design, a metamaterial surface with numbers of metal nails are embedded into the bottom of the waveguide cavity to achieve the filtering response, where slots are opened on the waveguide broad-wall to realize frequency resonance and energy radiation of the antenna array. Such structure has the advantages of simple structure, easy manufacturing and large stop-band range. However, several amounts of energy is easily retained in the gaps among the large number of metal nails, which has been verified a large insertion loss exists in this structure and finally results in a poor transmission performance.

In this paper, in order to alleviate the above-mentioned technical problems, a new type of filtering waveguide is proposed and realized with the help of 3D printing technique. Unlike the structures of the previous works, the presented design has a much simpler structure and lower loss, and the pass-band and stop-band can be easily adjusted to meet different application requirements.

II. CONSTRUCTION OF FILTERING WAVEGUIDE

The construction of the proposed filtering waveguide is shown in Fig. 1. As different from a conventional waveguide with complete solid metallic walls, the designed structure possesses a metamaterial-based surface to take place of one of the broad-walls. The metamaterial-based surface is composed of periodic metallic bars. By employing such surface into the waveguide, the model is able to transmit a desired bandwidth of signal (pass-band) in the Ku-band while generating an out-of-band rejection (stop-band). In order to facilitate the experimental setup and test, two waveguide stepped transitions are designed to connect the two filtering waveguide ports with commercial coaxial-to-waveguide adapters. The structural parameters of the filtering waveguide shown in Fig. 1 are tabulated in Table 1, where a and b are the length and width of the rectangular waveguide respectively; w and h are the width and height of the metallic bars respectively; i is the interval among the metallic bars. Note that the length of the periodic bars is identical to the length of the waveguide broad-wall. In addition, I structure of the waveguide stepped transition is shown in Fig. 2. The transition is composed of four steps. Its structural parameters are tabulated in Table 1, where (b, b_1, b_2 and b_3) and (c_0, c_1, c_2, and c_3) are the heights and widths of the four steps respectively.

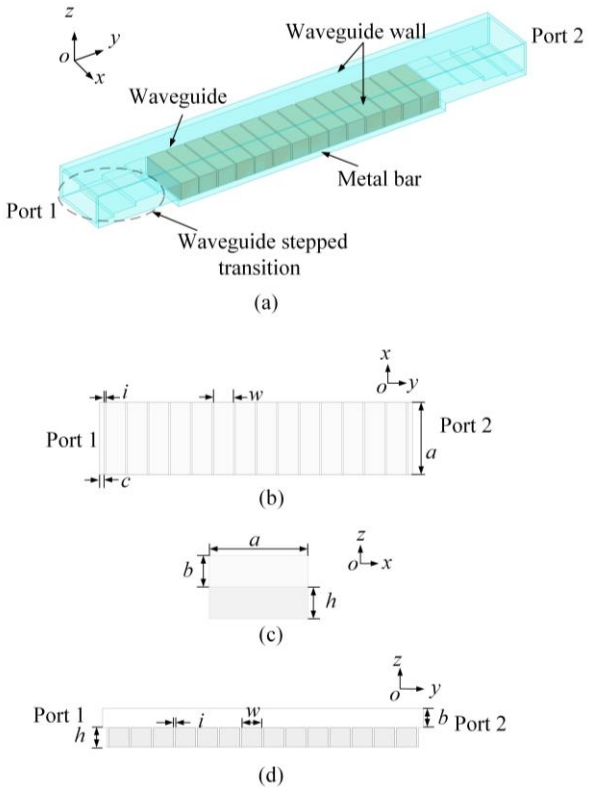

Fig. 1. Structure of the designed filtering waveguide. (a) 3D-view of the whole filtering waveguide. (b) Top-view of the filtering waveguide. (c) Front-view of the filtering waveguide. (d) Side-view of the filtering waveguide.

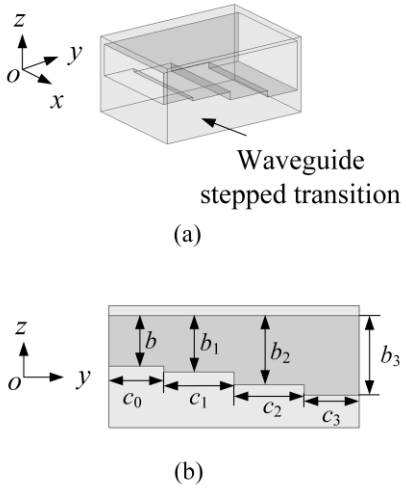

Fig. 2. Structure of the waveguide stepped transition. (a) 3D-view of the waveguide stepped transition. (b) Front-view of the waveguide stepped transition.

Table 1: Parameters of the filtering waveguide

Parameter	Value	Parameter	Value
a	15.79 mm	b_1	5.6 mm
b	5.06 mm	b_2	6.9 mm
c	1.2 mm	b_3	7.89 mm
w	5.5 mm	c_0	5.5 mm
h	4.8 mm	c_1	7.0 mm
i	0.7 mm	c_2	7.0 mm
-	-	c_3	5.5 mm

III. DESIGN AND ANALYSIS OF THE FILTERING WAVEGUIDE

A. Operational principle

According to EM theory, the electric-field (*E*-field) propagates vertically between two parallel perfect electric conductors (PECs) at any spacing. However, when one of the two parallel PECs is replaced by a perfect magnetic conductor (PMC), the EM wave propagation property would be changed. Once the distance between the two conductors (PEC and PMC) is less than quarter wavelength of the operating frequency, propagation of the *E*-field no longer exists, i.e., its cut-off frequency is higher than that of all propagation modes [13]. The periodic surface can create a cut-off band, which is realized theoretically by providing high surface impedance on the periodic structure, i.e., rendering it as an artificial magnetic conductor [13].

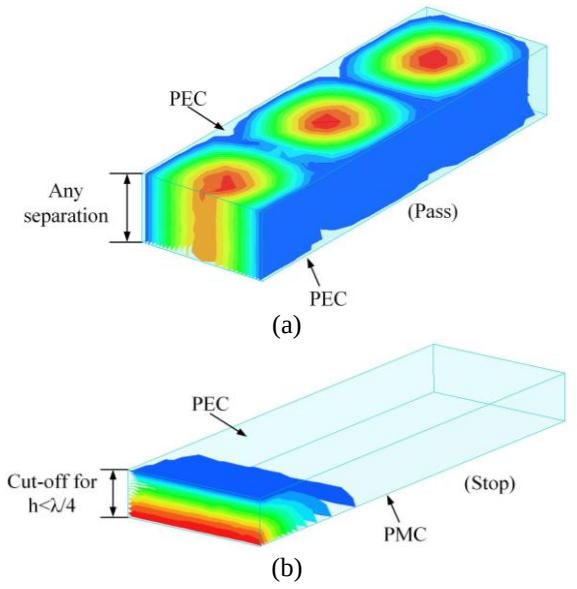

Fig. 3. *E*-field propagation of a waveguide with different constructions on the top and bottom surfaces. (a) A PEC top surface and a PEC bottom surface. (b) A PEC top surface and a PMC bottom surface.

According to the principle mentioned above, a metamaterial-based surface with a customized structure can be designed so that it can appear as a PEC surface in the interested frequency band where signals can be transmitted freely, while at the same time, it can also perform as a PMC surface in a specific frequency band where undesired signals will be blocked, as shown in Fig. 3. Therefore, a filtering function with pass-band and stop-band characteristics simultaneously is possible to be realized in a single waveguide.

B. Analysis of the filtering waveguide

According to the principle described in last sub-section, the filtering waveguide can be established in the form of the configuration as shown in Fig. 1. To properly realize the PEC and PMC functional transformation in desired and undesired frequency bands, a metamaterial-based surface consisting of periodic metallic bars is adopted and integrated to replace one of the waveguide broad-wall. The proposed filtering waveguide is designed in Ku-band operation. The EM model is analyzed and optimized in CST Microwave Studio® [14]. The transmission coefficient (characterized by S_{21}) of the designed filtering waveguide is shown in Fig. 4, from which one can observe that the S_{21} response of the waveguide in the bandwidth of 12.0 GHz~15.5 GHz, is almost the same as that of a traditional waveguide, i.e., S_{21} is close to 0 dB due to the low insertion loss of the waveguide structure. More specifically, the insertion loss is less than 0.1 dB from 12.0 GHz to 14.5 GHz with reflection coefficient (characterized by S_{11}) lower than -15 dB, which demonstrates good wave-propagation performance in the pass-band.

On the other hand, there is a large attenuation appearing in the bandwidth from 16.2 GHz to 17 GHz in the designed filtering waveguide, as shown in Fig. 4. The reason is traced to the phenomenon that the proposed metamaterial-based surface operates as a PMC layer at the bottom of the waveguide in this frequency band, so a stop-band is obtained.

To further illustrate the pass-band and stop-band performance of the proposed filtering waveguide, the *E*-field distribution at different frequencies inside the waveguide is shown in Fig. 5. In addition, the operating pass-band and stop-band of the filtering waveguide can be easily adjusted via properly choosing the parameters of the metamaterial-based surface. For instance, the height (h) and the width (w) of the metallic bars can be tuned to meet different requirements. As shown in Fig. 6, the stop-band moves to lower frequency band as the height of the metallic bar becomes larger while the other parameters are kept unchanged. Similarly, as the width of the metallic bar increases, the stop-band becomes wider and shifts slightly to the lower frequency band at the same time. All of the above analysis verifies the proposed structure is a simple but efficient approach to function a desired filtering response in a waveguide.

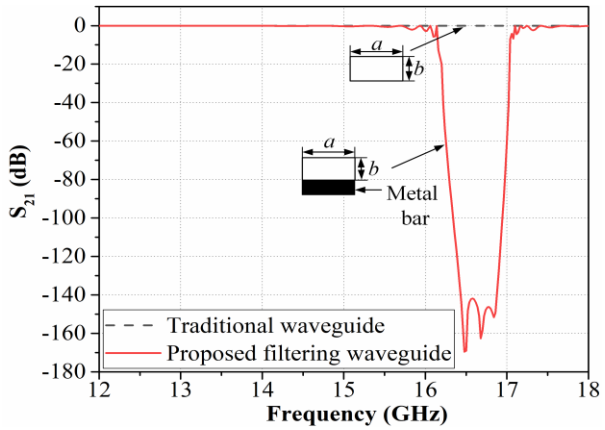

Fig. 4. Simulated S_{21} of the filtering waveguide and traditional waveguide.

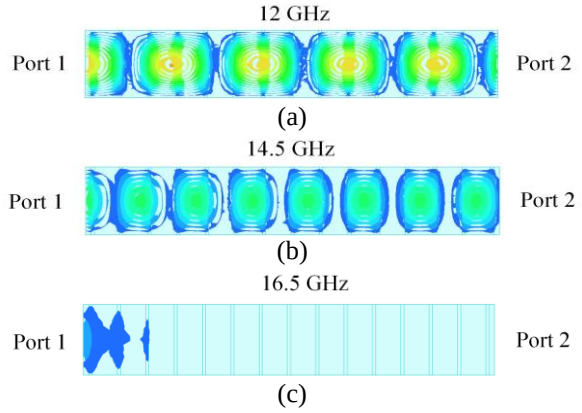

Fig. 5. Top-views of the electric-field distribution in the proposed filtering waveguide at different frequencies.

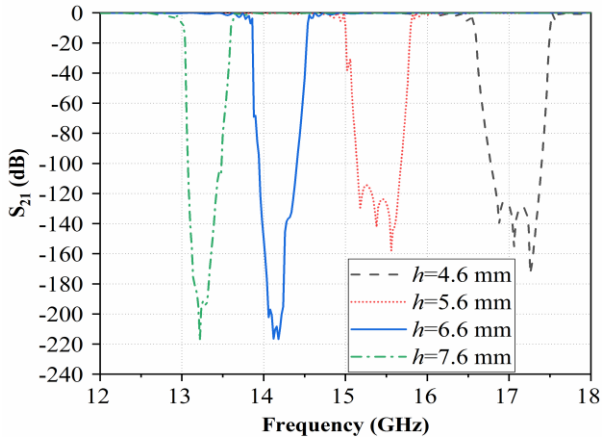

Fig. 6. Effect of various metallic bars' heights on the filtering waveguide.

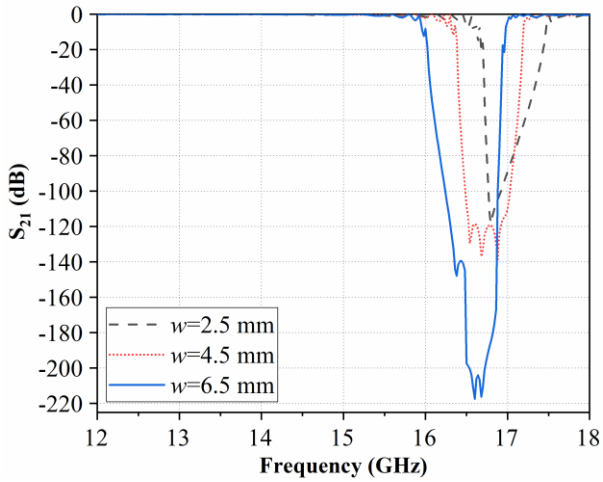

Fig. 7. Effect of various metallic bars' widths on the filtering waveguide.

IV. EXPERIMENTAL RESULTS

To prove the feasibility of the proposed filtering waveguide, a prototype waveguide has been fabricated by using 3D printing technology and tested with vector network analyzer (VNA) in laboratory. The prototype is 3D printed in aluminum via the metal printing process called direct-metal-laser-sintering (DMLS) [15], [16], which can greatly reduce or even eliminate any assembly and alignment errors from traditional machining process. The final test model is assembled by the proposed waveguide and two standard WR-62 coaxial-to-waveguide adaptors at both ends of the waveguide, as shown in Fig. 8. The measured S-parameters results of the filtering waveguide is presented in Fig. 9. As can be seen from the figure, the measured results are in good agreement with the simulated ones obtained from simulation environment. The pass-band and stop-band are roughly locating at the same range as the simulation, indicating that the designed filtering waveguide is indeed feasible in a compact waveguide volume. In addition, from the test results, it is observed that the stop-band is slightly narrower than the simulated one, which is mainly caused by minor tolerances on certain key structural parameters of the metallic bars during the DMLS manufacturing process. At the same time, as the internal surface and structure of the prototype are hard to polish while a planar surface with PEC surface is set in simulation, some uneven places can be observed in the waveguide, which introduces several amount of insertion loss into the filtering performance. Further fine post-processing on the surface roughness of the prototype will help improve the filtering response.

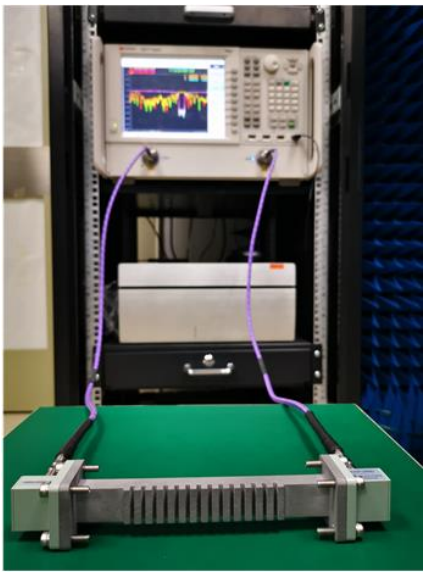

Fig. 8. The prototype waveguide in test environment.

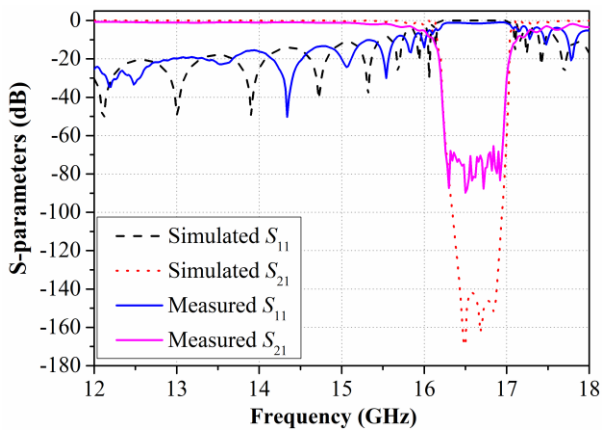

Fig. 9. Simulated and measured S-parameters of the filtering waveguide.

V. CONCLUSION

A new type of filtering waveguide is proposed in this work. The filtering waveguide is configured by a conventional rectangular waveguide and periodic metallic bars as the metamaterial-based surface, functioning as a PEC in pass-band while PMC in stop-band. The operating principle and design process have been illustrated. A 3D printed prototype was tested and the overall test results well agree with the simulated ones. The proposed design is also easily for customizing to different frequency bands' application by adjusting certain structural parameters, which makes it more applicable to various advanced communication systems.

ACKNOWLEDGMENT

This work was supported partially by the State Key Laboratory of Millimeter Waves under Grant No. K201932, the National Taipei University of Technology-Shenzhen University Joint Research Program under Grant No. 2020011, the Fok Ying-Tong Education Foundation, China under Grant No. 171056, the National Natural Science Foundation of China under Grants 61801300 and 61701320, and the New Teacher Natural Science Research Project of Shenzhen University under Grant No. 860-000002110627. The authors would like to express our sincere thanks to Dr. Vincent Zhang for his valuable suggestion during the research progress of the work.

REFERENCES

[1] J. Jiang, Y. Xia, and Y. Li, "High isolated X-band MIMO array using novel wheel-like metamaterial decoupling structure," *Applied Computational Electromagnetics Society Journal*, Accepted, vol. 34, no. 12, pp. 1829-1836, 2019.

[2] F. Liu, J. Guo, L. Zhao, G. L. Huang, Y. Li, and Y. Yin, "Dual-band metasurface-based decoupling method for two closely packed dual-band antennas," *IEEE Transactions on Antennas and Propagation*, vol. 68, no. 1, pp. 552-557, Jan. 2020.

[3] G.-L. Huang, J. Liang, L. Zhao, D. He, and C.-Y.-D. Sim, "Package-in-dielectric liquid patch antenna based on liquid metal alloy," *IEEE Antennas and Wireless Propagation Letters*, vol. 18, no. 11, pp. 2360-2364, Nov. 2019.

[4] J. Li, X. Zhang, Z. Wang, X. Chen, J. Chen, Y. Li, and A. Zhang, "Dual-band eight-antenna array design for MIMO applications in 5G mobile terminals," *IEEE Access*, vol. 7, pp. 71636-71644, 2019.

[5] F. Liu, J. Guo, L. Zhao, G. Huang, Y. Li, and Y. Yin, "Ceramic superstrate-based decoupling method for two closely packed antennas with cross-polarization suppression," *IEEE Transactions on Antennas and Propagation*, Submitted.

[6] J. Guo, F. Liu, L. Zhao, Y. Yin, G. Huang, and Y. Li, "Meta-surface antenna array decoupling designs for two linear polarized antennas coupled in H-plane and E-plane," *IEEE Access*, vol. 7, pp. 100442-100452, 2019.

[7] L. Zhao, G. Jing, G.-L. Huang, W. Lin, and Y. Li, "Low mutual coupling design for 5G MIMO antennas using multi-feed technology and its application on metal-rimmed mobile phones," *IEEE Transactions on Antennas and Propagation*, Submitted.

[8] Q. Wu, F. Zhu, Y. Yang, and X. Shi, "An effective approach to suppressing the spurious mode in rectangular waveguide filters," *IEEE Microwave and Wireless Components Letters*, vol. 29, no. 11, pp. 703-705, Nov. 2019.

[9] V. G. Veselago, "The electrodynamics of substances with simultaneously negative values of ε and μ,"

Sov. Phys.-Usp., vol. 10, no. 4, pp. 509-514, Jan.-Feb. 1968.

[10] A. Yelizarov, I. Nazarov, A. Skuridin, and A. Kukharenko, "Investigation of a rectangular waveguide with a magnetic wall made of mushroom-shaped metamaterial," *2017 Eighteenth International Vacuum Electronics Conference (IVEC)*, London, pp. 1-3, 2017.

[11] A. A. Yelizarov, I. V. Nazarov, T. V. Sidorova, O. E. Malinova, and V. N. Karavashkina, "Modeling of a waveguide stop-band filter with a mushroom-shaped metamaterial wall and dielectric substrates," *2018 Systems of Signal Synchronization, Generating and Processing in Telecommunications (SYNCHROINFO)*, Minsk, pp. 1-3, 2018.

[12] W. Wang, *et al.*, "A waveguide slot filtering antenna with an embedded metamaterial structure," *IEEE Transactions on Antennas and Propagation*, vol. 67, no. 5, pp. 2953-2960, May 2019.

[13] P.-S. Kildal, A. U. Zaman, E. Rajo-Iglesias, E. Alfonso, and A. Valero-Nogueira, "Design and experimental verification of ridge gap waveguide in bed of nails for parallel-plate mode suppression," *IET Microwaves, Antennas & Propagation*, vol. 5, no. 3, pp. 262-270, Feb. 21, 2011.

[14] CST Microwave Studio, Dec. 2019. [Online] Available: https://www.cst.com/

[15] G.-L. Huang, C.-Z. Han, W. Xu, T. Yuan, and X. Zhang, "A compact 16-wayhigh-power combiner implemented via 3-D metal printing technique for advanced radio-frequency electronics system applications," *IEEE Transactions on Industrial Electronics*, vol. 66, no. 6, pp. 4767-4776, Jun. 2019.

[16] G.-L. Huang, S.-G. Zhou, and T. Yuan, "Design of a compact wideband feed cluster with dual-polarized sum- and difference-patterns implemented via 3-D metal printing," *IEEE Transactions on Industrial Electronics*, vol. 65, no. 9, pp. 7353-7362, Sept. 2018.